Neuron, Volume *80*

Supplemental Information

A Tale of Two Retinal Domains: Near-Optimal Sampling of Achromatic Contrasts in Natural Scenes through Asymmetric Photoreceptor Distribution

Tom Baden, Timm Schubert, Le Chang, Tao Wei, Mariana Zaichuk, Bernd Wissinger, and Thomas Euler

Supplemental Figures

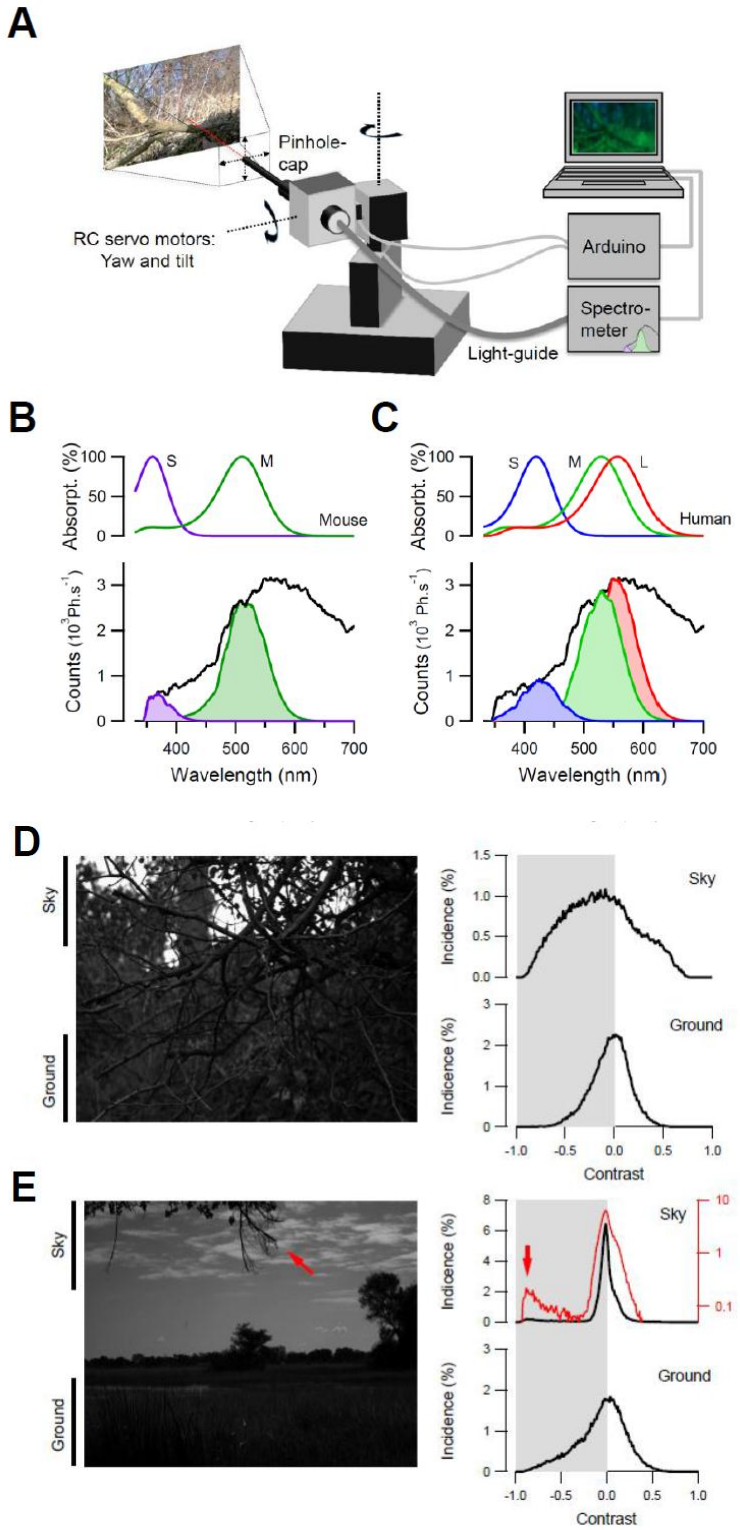

Figure S1 | Sampling and calculation of natural statistics in visual scenes – related to Figure 1.

A, Schematic of the "hyperspectral-scanner", built from a UV-capable spectrometer (USB2000+VIS-NIR, Ocean Optics, Ostfildern, Germany) and two generic-brand RC-servo motors rotating the optical fibre (light guide, core diameter: 200 µm) of the spectrometer in yaw and tilt. "Pixel size" was defined by the aperture of a pinhole cap attached to optical fibre. The RC servos were driven by an open-source microprocessor board (http://arduino.cc), controlled by the computer that also acquired the spectra. **B**,**C**, absorption spectra of mouse (B, *top*) and human (C, *top*) opsins and example for calculation of relative opsin activation from spectra recorded at a single image "pixel" (*bottom*). **D,E,** Greyscale images of "human view" natural scenes taken from a public database (Tkačik et al., 2011) and contrast distribution in sky and ground. The branch covering the sky in (E, red arrow) gives rise to a small peak at negative contrasts (red, same as black trace but plotted on a log scale) next to a comparatively narrow contrast distribution in the remainder of the sky.

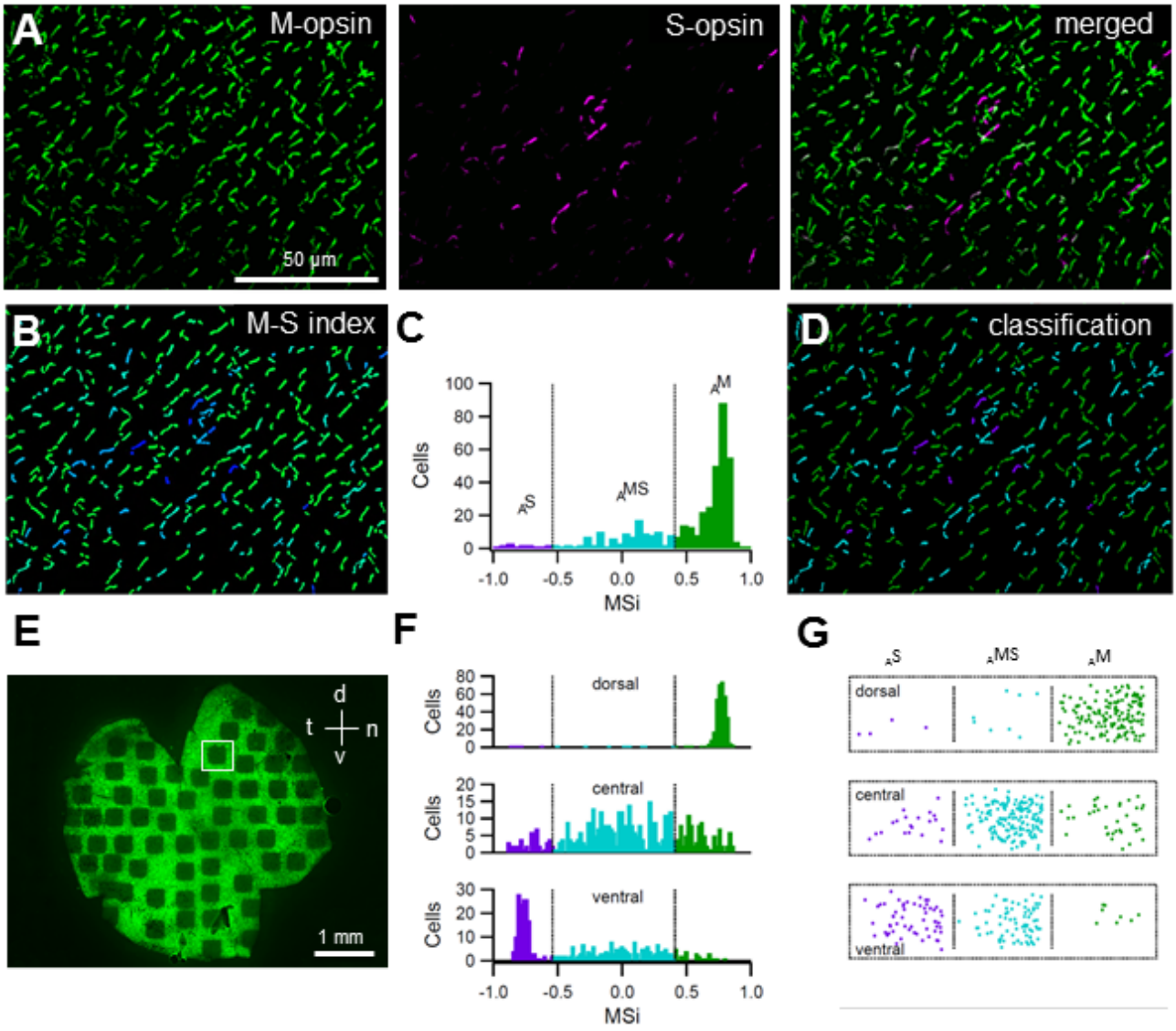

Figure S2 | Semi-automated analysis of immunolabelled cone photoreceptor outer segments – related to Figure 2.

A, flat-mounted HR2.1:TN-XL retina labelled with antibodies against M and S opsin. **B**, immunolabelled cone outer segments detected by Laplacian operator (see Experimental Procedures), colour coded by "M-S index" (MSi) and **C**, histogram of MSi calculated from (A). **D**, distribution of anatomical cone types based on MSi threshold definition: $_{A}$M, $_{A}$S and $_{A}$MS cones (in green, purple and cyan, respectively). **E**, fluorescence image (GFP) of an entire retina with bleach zones where individual high-resolution images as shown in (A) had been taken; white box denotes position of images shown in (A,B,D). **F**, MSi histograms of representative dorsal, central and ventral regions and **G**, spatial distribution of detected cone types separated by MSi-based anatomical classification. Note: cones expressing either M or S opsin

in theory yield an MSi near 1 or -1, respectively. However, as positive versus background fluorescence in opsin stainings was normalised to a mean S/N ratio of 8:1, MSi values for "pure" M and S cones peak around 0.75 and -0.75 (F). MS cones, which co-express both opsins, yield an MSi around 0. Separations between anatomical M, S, and MS cones ($_{A}$M, $_{A}$S, $_{A}$MS) were defined based on the minima of a sum-of-3-gaussian-fit to the MSi histogram from n=39,916 cones analysed in 137 fields of view from 3 retinas (Fig. 2A_2, taken from (E), cf. Fig. 2C; thresholds: -0.54 and 0.41; see also *Assessing quality of cone type distribution fits*, *Methods*). Notably, the assumption of putative differences in binding affinity of the antibodies against S and M opsin has no impact on the separation of MSi peaks, but only results in numerical differences (skew) in the MSi distribution (data not shown). Therefore the separation of the three anatomical cone types based on MSi thresholds is independent of the actual relative antigen binding affinities of the opsin antibodies.

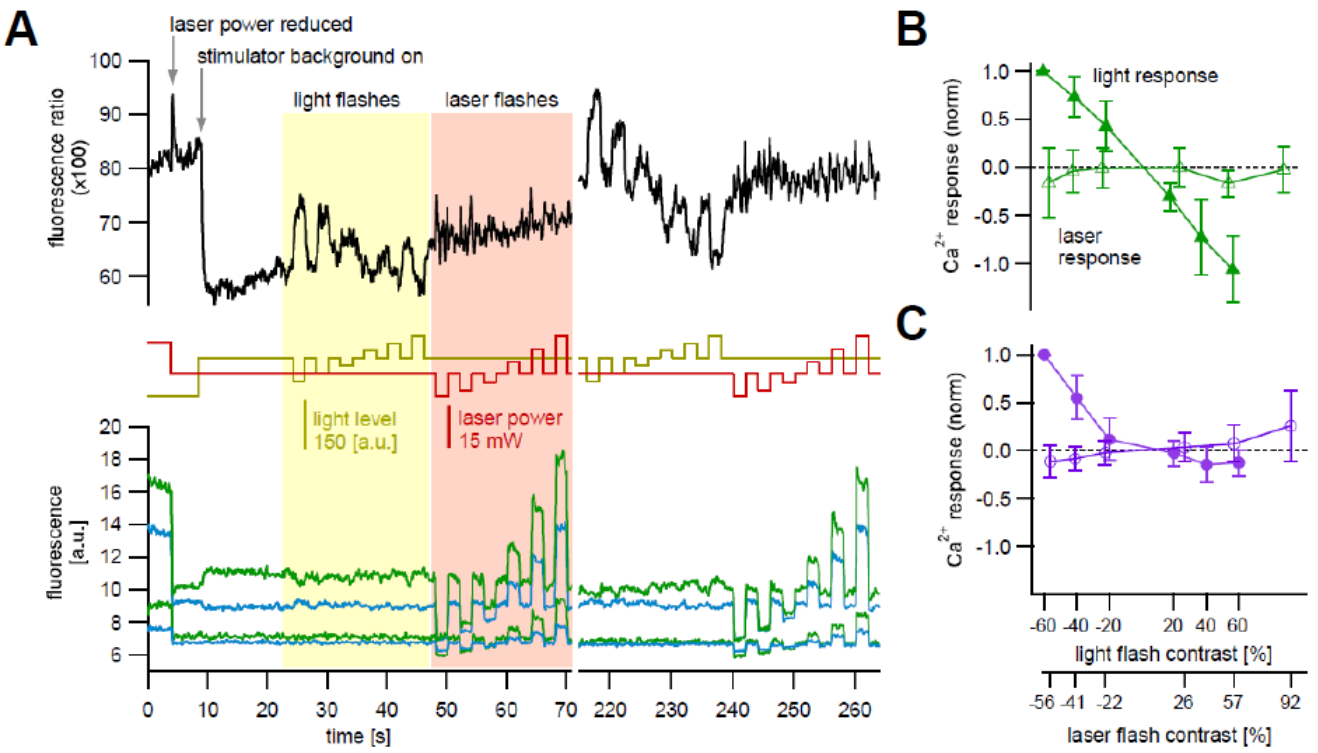

Figure S3 | Effect of 2P excitation laser on Ca^{2+} signal in cone terminals – related to Figure 3.

A, *top:* Ca^{2+} signal recorded in the axon terminals of functional M cones ($_{F}$M, dorsal retina) using 2P microscopy (black trace, ratio of citrine/EGFP fluorescence as reported by TN-XL, average of 8 cells). *Centre*: light stimulus (yellow trace, both S and M opsins were excited at the same photoisomerisation rate, "mouse white"-stimulus) and 2P excitation laser power (red trace, λ=860 nm). *Bottom*: fluorescence signals of the two TN-XL fluorophores, citrine (green) and EGFP (cyan); lower trace pair represents background fluorescence (in region of interest outside the cones). Reducing the laser power at the beginning of the recording elicited a transient in the ratio (Ca^{2+}) signal but had no persistent effect; the transient was at least partially caused by switching of the electronic circuitry that controlled the Pockels cell, which modulates the laser power. Turning on the stimulator LEDs (to background level) evoked a strong decrease in Ca^{2+} signal (light response). The cones responded to both dark and bright 2 s "flashes" (same intensity range as in our study) but only weakly to decreasing and increasing steps in excitation laser power (~6 to 28 mW as measured under the objective lens; typically used for recordings: 5-15 mW). Note that the laser steps are strongly reflected in citrine and EGFP fluorescence, but hardly in the ratio (Ca^{2+}) signal. **B**, normalized Ca^{2+} responses measured in n=12 $_{F}$M cones (dorsal retina) as a function of stimulus (solid symbols) or laser power contrast (open symbols); same protocol as in a (area under curve,

calculated for the centre 1.5 s of each response to avoid potential switching artefacts and normalized to the highest contrast dark flash response, ± s.d.). **C**, as B but for n=14 $_{F}$S cones (ventral retina). The responses evoked by laser flashes were not significantly different between $_{F}$M and $_{F}$S cones, except for the two highest laser flash contrasts (-56% p=0.77; -41% p=0.17; -22% p=0.96; 26% p=0.47; 57% and 92% p<0.05; t-Test).

In an earlier study (Euler et al., 2009), the effect of the 2P excitation laser on (electrically recorded) retinal ganglion cell activity was investigated in wholemount preparations. The largest laser-evoked contribution came from direct 2P photopigment excitation (equivalent to ~$2 \cdot 10^4$ P*s^{-1}/rod, for λ_{LASER} = 930 nm @ 5 mW), while direct 1P excitation was ~1000 times lower. The fluorescence generated in the scan field also contributed to laser-evoked activity but strongly depended on the fluorescence intensity (i.e. fraction of fluorescent structures in the scan field) and was estimated to be ~300 times lower than the 2P contribution (for details on calculations, see Euler et al., 2009).

In the present study, we used vertical slices instead of wholemounts: By restricting the laser scanning to a region covering solely cone terminals (Wei et al., 2012), the perpendicular orientation of the laser beam to the slice surface prevented direct in-path laser illumination of the photopigments. Therefore only scattered laser light could reach the photopigments. Since 2P events require two photons reaching a fluorophor virtually at the same time (Denk et al., 1990; Göppert-Mayer, 1931), 2P photopigment excitation from scattered laser light seems less likely. However, since in the wholemount, substantial 2P excitation of photopigment was observed even at a distance of several tens of µm distant from the focal plane (Euler et al., 2009), a 2P excitation component in the slice configuration cannot be excluded. That (scattered) laser light caused 1P photopigment excitation is possible but (due to the perpendicular orientation of the laser beam) expected to be lower than in the wholemount situation. Fluorescence generated in the scan field may have caused similar laser-evoked effects in slices and wholemounts, and due to the TN-XL emission wavelengths around ~500 nm fluorescent light is expected to affect M opsin more strongly than S opsin. For two reasons we think that this bias is not relevant for our measurements: First, we used as little laser power as possible to get reliable signals and kept the fluorescent structures in the scan field to a minimum (a strategy that is quite effective, cf. Fig. 8a in Euler et al., 2009). Second, for the laser power range used in our study the weak responses cause by laser flashes were not significantly different for $_{F}$S and $_{F}$M cones (see above).

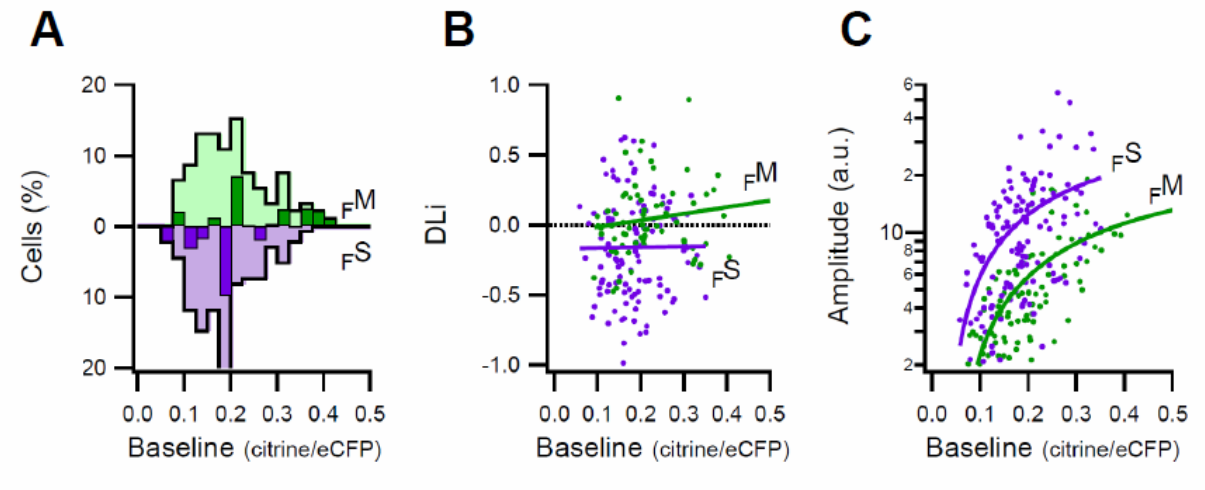

Figure S4 | No effect of baseline Ca^{2+} on contrast coding – related to Figure 6.

A, distribution of baseline Ca^{2+} levels (as ratio $R=F_A/F_D$, see Supplementary Fig. S2 and Experimental Procedures) of $_F$M and $_F$S cones evaluated in Fig. 6B,E ($p>0.05$). **B**, dark-light index (DLi) was independent of baseline Ca^{2+} level ($p<0.001$) whereas **C**, amplitude was positively correlated with baseline Ca^{2+} level (rho=0.67).

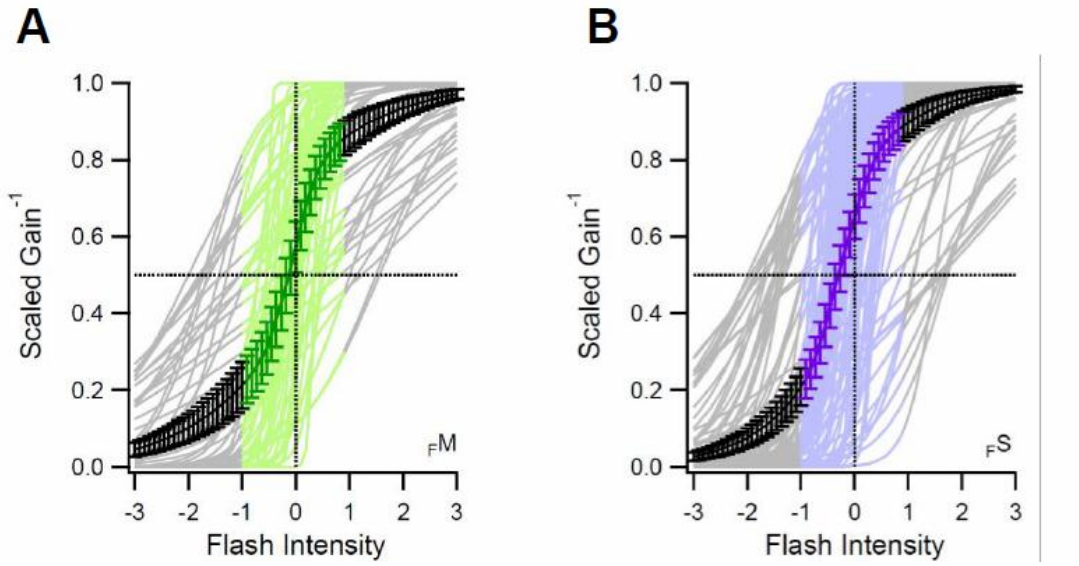

Figure S5 | Coding optimisation and Ideal Observer Analysis

– related to Figure 7.

A,**B**, individual gain functions of $_{F}$M (a, green) and $_{F}$S (b, purple) cones (dataset from Fig. 6B,C). Gain functions are amplitude-normalised to saturation points determined by extrapolation of the sigmoidal fit (grey), error: 95% confidence limits.

Supplemental Reference

Göppert-Mayer, M. (1931). Über Elementarakte mit zwei Quantensprüngen. Annals of Physics (Paris) *9*, 273-295.